PERGAMON

Solid State Communications 114 (2000) 59–62

solid state communications

www.elsevier.com/locate/ssc

Magnetic behavior of zero-field-frozen ferrofluid

P.C. Morais[a,*], C.B. Teixeira[a], K. Skeff Neto[a], R.B. Azevedo[b], Z.G.M. Lacava[b], L.M. Lacava[b]

[a]*Instituto de Física, Núcleo de Física Aplicada, Universidade de Brasília, C.P. 04455, CEP 70919-970 Brasília (DF), Brazil*
[b]*Departamento de Genética e Morfologia, Instituto de Biologia, Universidade de Brasília, 70910-900 Brasília (DF), Brazil*

Received 11 November 1999; accepted 7 January 2000 by C.E.T. Gonçalves da Silva

Abstract

In contrast to the spin glass-like state described in the literature, an alternative approach to explain the temperature dependence of the magnetization in a zero-field-frozen ferrofluid (ZFFF) is proposed in this work. It is claimed that the presence of a well-defined peak in the magnetization (M) versus temperature (T) curve results from the following combined effects: the temperature dependence of the reorientation of the magnetic moment associated to the nanomagnetic particle, saturation magnetization and magnetic anisotropy. The sample used in this work is a Nickel ferrite-based ferrofluid, which was investigated using magnetometry and transmission electron microscopy, the latter indicating the presence of nanomagnetics with a mean particle diameter of 11.1 nm and standard deviation of 0.37. Excellent agreement between theory and experiment is found for the M vs T curve using the ferrofluid sample containing 3×10^{16} particle/cm^3 and submitted to magnetic fields of 1, 3 and 5 kG.

Keywords: A. Nanostructures; B. Chemical synthesis; C. Scanning and transmission electron microscopy; D. Order–disorder effects

Material systems composed of magnetic nanoparticles dispersed in a nonmagnetic matrix are of great current interest. From the practical point of view, the interest spans from the development of high-density storage media, where spontaneous magnetization reversal determines the efficiency of the stored information [1], to the development of biocompatible ferrofluids, where the application of low-amplitude alternated magnetic fields may cause cancer cell disruption [2]. As far as the theoretical aspect is concerned, magnetic nanoparticles immersed in nonmagnetic material media can be used to investigate the competing dipolar interaction combined with random anisotropy. Mean-field calculation has shown that weak local anisotropy would destroy the long-range magnetic order, giving rise to a glass-like phase at high temperatures [3]. This theoretical result has been experimentally confirmed in highly anisotropic dysprosium (Dy) alloys [4]. The magnetization (M) versus temperature (T) curve of zero-field-cooled (ZFC) Dy alloys shows a sharp cusp at low temperature [5]. The cusp observed in the ZFC Dy alloys has been taken as the signature of the onset of a spin glass-state [6,7]. Magnetic nanoparticles dispersed in nonmagnetic matrices and cooled down to low temperatures under zero magnetic field condition also present a well-defined cusp in the M vs T curve [8,9]. Likewise, investigation of the magnetic properties of zero-field-frozen ferrofluids (ZFFF) shows a well-defined peak in the M vs T curve [10–12]. The peak temperature in ZFFF depends upon both the nanomagnetic particle concentration and the applied magnetic field (H) used in the course of the magnetization measurements. The peak temperature increases with increasing applied field for low-fields (below 100 G) and decreases with increasing applied field for high-fields (above 100 G) [10]. Further, the peak temperature increases monotonically with the nanoparticle concentration [11,12]. In the ZFFF the M vs T data have been only qualitatively discussed in terms of a spin glass-like behavior where dipole–dipole interaction is supposed to dominate the magnetic properties at low fields while uniaxial anisotropy dominates at high fields [10–12]. A local-mean-field study has been performed to explain the ZFFF data, though it reproduces qualitatively the main features only at high magnetic fields [13]. Nevertheless, little investigation has been performed with ZFFF despite the current interest in their magnetic properties. The present

* Corresponding author. Tel.: + 55-61-273-6655; fax: + 55-61-272-3151.

E-mail address: pcmor@fis.unb.br (P.C. Morais).

0038-1098/00/$ - see front matter
PII: S0038-1098(00)00021-1

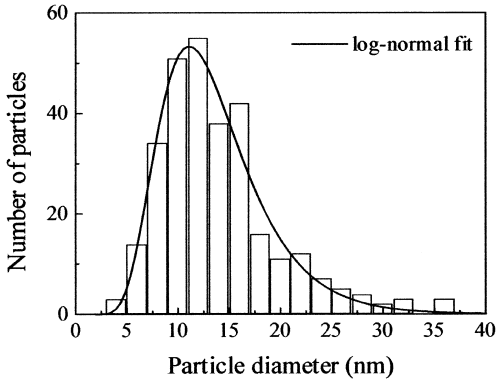

Fig. 1. The $NiFe_2O_4$ particle size histogram as obtained from transmission electron microscopy.

work discusses quantitatively the M vs T curve of ZFFF in the high magnetic field regime (above 100 G) in terms of a simple model. It will be shown that an alternative explanation, not based on spin glass theories, is successfully used to explain the experimental data obtained with a nickel ferrite-based ionic ferrofluid, in a wide range of temperatures. The success of the single-particle approximation used here was previously predicted by Shliomis et al. [14], who stressed that magnetic relaxation mechanisms rather than a phase transition to a magnetically ordered state or to a dipole glass state, would explains the peculiarities of the magnetization of ferrofluids.

Ferrofluids are ultra-stable colloidal systems composed of subdomain magnetic nanoparticles dispersed in organic or inorganic carrier fluids. In particular, ionic ferrofluids are water-based ferrofluids, stable under both low pH (acid ferrofluids) and high pH (basic ferrofluids) condition [15]. Because ferrofluids can be continuously diluted by solvent

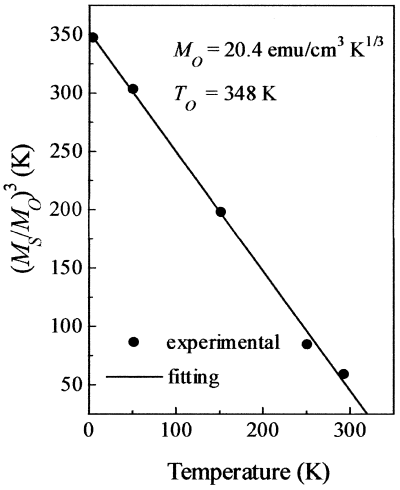

Fig. 2. Reduced saturation magnetization (M_S/M_0) versus temperature (T) for the nickel ferrite-based ferrofluid sample.

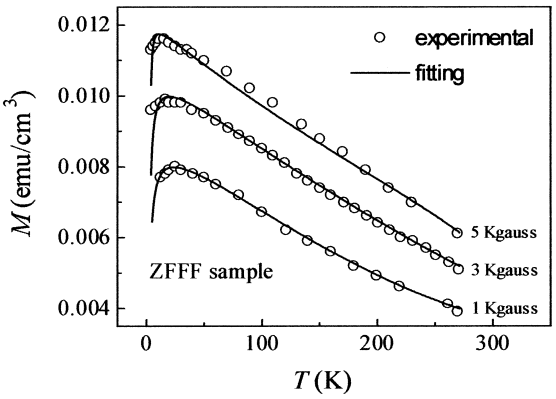

Fig. 3. Temperature (T) dependence of the magnetization (M) for the zero-field-frozen ferrofluid sample (open circles). Different values of external fields (1, 3 and 5 kG) were used to obtain the zero-field-frozen magnetization curves. The solid lines represent the best fitting according to the model discussed in this work.

addition, they represent the ideal material system to investigate the competing dipolar interaction combined with random anisotropy. The ferrofluid stability is achieved through a combination of particle thermal motion and particle–particle repulsion, both working against a magnetic dipole and van der Waals' interaction that tends to stick particles together. Steric repulsion prevents particle agglomeration in surfacted ferrofluids [16] while coulombic repulsion accounts for the stability in ionic ferrofluids [17,18]. The nickel ferrite-based ($NiFe_2O_4$) ionic ferrofluid sample used here has been synthesized using the chemical condensation of Ni^{2+} and Fe^{3+} ions in alkaline medium [19]. The magnetic nanoparticle concentration was set around 3×10^{16} particle/cm^3, through dilution from the initial sample. The particle size polydispersity parameters, i.e. the mean particle diameter (11.1 nm) and the standard deviation of the distribution (0.37) were obtained using transmission electron microscopy (TEM). The particle size histogram obtained from the TEM data was fitted using the standard approach, i.e. the log-normal distribution function, as shown in Fig. 1 [20]. The magnetization measurements were performed in the range of 4.2–293 K using a commercial VSM system, previously calibrated with a nickel-standard sample. Full points in Fig. 2 show the temperature dependence of the normalized saturation magnetization (M_S/M_0). In order to obtain the M vs T curves, the nickel ferrite ferrofluid sample was first cooled in a zero magnetic field from room temperature to 4.2 K. Previous magnetic resonance investigation showed that this sample freezes around 260 K with no indication that flocculation takes place [21]. After the cooling process, a steady magnetic field was applied to the sample and the magnetization measurements were performed while the temperature was increased. Steady fields of 1, 3 and 5 kG were used during the M vs T measurements. Open circles in Fig. 3 represent the temperature dependence of the magnetization of the $NiFe_2O_4$ ZFFF

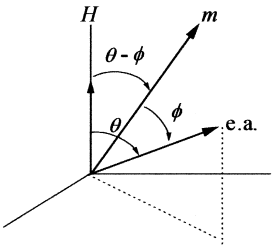

Fig. 4. Schematic representation of the relative orientation of the external applied field (H), easy axis (e.a.) and magnetic moment (m).

sample, being qualitatively identical to the results obtained with ferrofluids based on Fe_3O_4 [10,11] and γ-Fe_2O_3 [12]. The errors involved in the measurement of the temperature and magnetization are of the order of 0.01 K and 0.0004 emu, respectively.

The model used in the present work to fit the ZFFF data starts with the calculation of the magnetization (M) of a randomly oriented ensemble containing N identical magnetic nanoparticles per unit volume bearing a magnetic moment (m) and frozen in a nonmagnetic matrix. Though the polydispersity of the sample is not included in the calculation, the non-rigid magnetic dipole approximation is taken into account. The frozen ensemble is then submitted to an external magnetic field of 1, 3 and 5 kG which leads to an angular distribution of the magnetic moment (m) of the particle with respect to both the external field (H) and the easy axis (e.a.), as shown schematically in Fig. 4. Under the applied magnetic field, the sample magnetization would be calculated as

$$M(T) = \sum_i m_i \cos(\theta_i - \phi_i),$$

where m_i is the magnetic moment associated to the ith particle. Note that the summation performed to obtain $M(T)$ is done over the N particles per unit volume. Assuming the N particles bearing the average magnetic moment m, the magnetization reads [22]

$$M(T) = Nm\langle\cos(\theta - \phi)\rangle, \quad (1)$$

where $\langle\ \rangle$ means statistical average. The temperature dependence of $M(f)$ is described here in terms of the product of Nm by $\langle\cos(\theta - \phi)\rangle$. To calculate $\langle\cos(\theta - \phi)\rangle$ we start writing the free energy (E) of the nanoparticle as $E = KV \sin^2\phi - mH\cos(\theta - \phi)$, where K and V are the magnetic anisotropy and the particle volume, respectively. Note that the particle–particle interaction is neglected in the description of the free energy (E). This approximation is supported by earlier experiments where particle–particle interaction only plays a marginal role on the M vs T curves, at high magnetic fields [10]. The relationship involving θ and ϕ, namely

$$\theta = \phi + \arcsin\left[\frac{KV}{mH}\sin(2\phi)\right]$$

is obtained at the free energy minimum condition. The $\langle\cos(\theta - \phi)\rangle$ term is then calculated by

$$\langle\cos(\theta - \phi)\rangle = \frac{\int_0^\pi \cos(\theta - \phi)\sin\phi\exp(-E/kT)\,d\phi}{\int_0^\pi \sin\phi\exp(-E/kT)\,d\phi}. \quad (2)$$

On the other hand, the temperature dependence of the saturation magnetization per unit volume ($M_S = Nm$) is usually described by [23]:

$$M_S = M_0(T_0 - T)^\beta. \quad (3)$$

Note that the best fit of the experimental data shown in Fig. 2 (full line) was obtained using Eq. (3) with $M_0 = 20.4$ emu/cm$^3 \times$ K$^{1/3}$, $T_0 = 348$ K and $\beta = 0.33$. Eqs. (2) and (3) are then used in Eq. (1) to fit the M vs T data of the ZFFF sample (see Fig. 3). Note that our fitting procedure of the M vs T data in Fig. 3 only takes into account the temperature dependence of the magnetic anisotropy (K). This is done numerically through the optimization of the M vs T curve using the best value of the magnetic anisotropy at each experimental point. In Fig. 5, open circles represent the temperature dependence of the magnetic anisotropy as a result of the fitting of the 3 kG ZFFF data from this paper, while full circles represent the temperature dependence of the magnetic anisotropy as reported for bulk $NiFe_2O_4$ samples [24]. According to our fitting procedure, we estimated the errors involved in the determination of the magnetic anisotropy to be of the order of 0.05×10^5 erg/cm^3. The shift observed in Fig. 5 between full and open circles is probably due to differences in nature of the samples (nanoparticles and bulk material). Indeed, the solid lines going through the points in Fig. 3 represent the best fit of the experimental M vs T points using Eq. (1) after taking into account Eqs. (2) and (3) and the temperature dependence of the magnetic anisotropy (see open circles in Fig. 5). At this point, a final comment concerning the particle

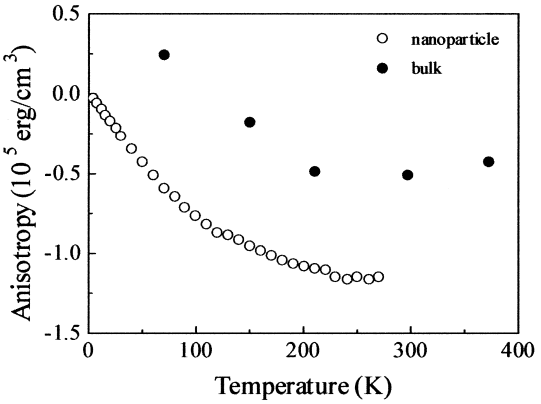

Fig. 5. Temperature dependence of the magnetic anisotropy as reported by Healy (full circles) [24] and from the present fitting procedure at 3 kG (open circles).

polydispersity and its influence on the analysis performed here may be of interest. Despite of the well-known influence of the particle polydispersity on the magnetic properties of ferrofluids we have not included it here, as discussed in what follows. A close analysis of Eq. (2) shows that the polydispersity enters in both the description of the free energy (E) and θ. However, the ratio $\alpha = KV/mH \propto K/M_S H$ is independent of V, and so is θ. Further, the free energy may be rewritten as $E = \alpha mH\{\sin^2 \phi - \alpha^{-1} \cos(\theta - \phi)\}$, indicating that the size dependence of E resides on m, which in turn is described by M_S/N through Eq. (3). Therefore, any size dependence of the magnetic moment associated to the nanoparticles in this particular sample is already included in the fitting of the experimental data shown in Fig. 2.

In conclusion, the temperature dependence of the magnetization of ZFFF based on $NiFe_2O_4$ is discussed in this work. The model used to explain the data includes the calculation of $\langle \cos(\theta - \phi) \rangle$ according to Eq. (2), the description of the saturation magnetization according to Eq. (3) and the assumption of a temperature dependence of the magnetic anisotropy. A few aspects concerning the experimental data and the approach used to explain the data deserve further comments. First, the description of the free energy includes only the anisotropy term and the Zeeman term. Though particle concentration was set at 3×10^{16} particle/cm^3 (about 2% volume fraction), the dipolar field due to neighbor nanoparticles seems to have a marginal effect compared to the external applied field, similar to what has been already reported for magnetite-based ferrofluids [10]. Second, though the visual aspect of the M vs T curve for ZFFF is quite similar to the visual aspect of the M vs T curve for ZFC Dy alloys, the model presented here is not based on any spin glass theory. Third, the model proposed here was not tested for low-field M vs T data, where the dipolar field is expected to play a central role for high and moderate values of nanoparticle volume fraction.

Acknowledgements

The Brazilian agencies FAPDF, PADCT, and CNPq supported this work.

References

[1] S. Morup, E. Tronc, Phys. Rev. Lett. 72 (1994) 3278.
[2] A. Jordan, P. Wust, R. Scholz, H. Faehling, J. Krause, R. Felix, in: U. Hafeli, W. Shutt, J. Teller, M. Zborowski (Eds.), Scientific and Clinical Applications of Magnetic Carriers, Plenum Press, New York, 1997, p. 569.
[3] A. Aharony, E. Pytte, Phys. Rev. Lett. 45 (1980) 1583.
[4] S. von Molnar, B. Barbara, T.R. McGuire, R.J. Gambino, J. Appl. Phys. 53 (1982) 2350.
[5] S. von Molnar, T.R. McGuire, R.J. Gambino, J. Appl. Phys. 53 (1982) 7666.
[6] R.V. Chamberlin, M. Hardiman, L.A. Turkevich, R. Orbach, Phys. Rev. B 25 (1982) 6720.
[7] G.G. Kenning, D. Chu, R. Orbach, Phys. Rev. Lett. 66 (1991) 2923.
[8] G. Xiao, S.H. Liou, A. Levy, J.N. Taylor, C.L. Chien, Phys. Rev. B 34 (1986) 7573.
[9] A. Gravin, C.L. Chien, J. Appl. Phys. 67 (1990) 938.
[10] W. Luo, S.R. Nagel, T.F. Rosenbaum, R.E. Rosensweig, Phys. Rev. Lett. 67 (1991) 2721.
[11] R.W. Chantrell, M. El-Hilo, K. O'Grady, IEEE Trans. Magn. 27 (1991) 3570.
[12] T. Jonsson, J. Mattsson, C. Djurberg, F.A. Khan, P. Nordblad, P. Svedlindh, Phys. Rev. Lett. 75 (1995) 4138.
[13] M.A. Zaluska-Kotur, M. Cieplak, Europhys. Lett. 23 (1993) 85.
[14] M.I. Shliomis, A.F. Pshenichnikov, K.I. Morozov, I. Yu, Shurubor, J. Magn. Magn. Mater. 85 (1990) 40.
[15] R. Massart, IEEE Trans. Magn. 17 (1981) 1247.
[16] S.E. Khalafalla, G.W. Reimers, US patent 3764540, 1973.
[17] R. Massart, US patent 4329241, 1982.
[18] P.C. Morais, F.A. Tourinho, G.R.R. Gonçalves, A.L. Tronconi, J. Magn. Magn. Mater. 149 (1995) 19.
[19] F.A. Tourinho, P.C. Morais, M.H. Sousa, L.G. Macedo, in: P.F. Gobin, J. Tatibouet (Eds.), Proceedings of the Third International Conference on Intelligent Materials and Third European Conference on Smart Structures and Materials (SPIE vol. 2779), p. 317.
[20] B. Payet, D. Vincent, L. Delaunay, G. Noyel, J. Magn. Magn. Mater. 186 (1998) 168.
[21] J.F. Saenger, K. Skeff Neto, P.C. Morais, M.H. Sousa, F.A. Tourinho, J. Magn. Magn. Mater. 134 (1998) 180.
[22] S. Morup, G. Christiansen, J. Appl. Phys. 73 (1993) 6955.
[23] P.C. Morais, K. Skeff, Neto, J. Appl. Phys. 58 (1985) 4336.
[24] D.W. Healy Jr., Phys. Rev. 86 (1952) 1009.